

Periodic windows distribution resulting from homoclinic bifurcations in the two-parameter space

R. O. Medrano-T.^{1,2} and I. L. Caldas²

¹ *Departamento de Ciências Exatas e da Terra, Universidade Federal de São Paulo, Diadema, São Paulo, Brasil and*
² *Instituto de Física, Universidade de São Paulo, São Paulo, Brasil*

Periodic solution parameters, in chaotic dynamical systems, form periodic windows with characteristic distribution in two-parameter spaces. Recently, general properties of this organization have been reported, but a theoretical explanation for that remains unknown. Here, for the first time we associate the distribution of these periodic windows with scaling laws based in fundamental dynamic properties. For the Rössler system, we present a new scenery of periodic windows composed by multiple spirals, continuously connected, converging to different points along of a homoclinic bifurcation set. We show that the bi-dimensional distribution of these periodic windows unexpectedly follows scales given by the one-parameter homoclinic theory. Our result is a strong evidence that, close to homoclinic bifurcations, periodic windows are aligned in the two-parameter space.

PACS numbers: 05.45.-a, 02.30.Oz, 05.45.Pq

Keywords: Homoclinic systems, Periodic windows, Bifurcation

I. INTRODUCTION

For several smooth nonlinear maps and differential equations, stable periodic orbits and their dependence on the system control parameters are well known. The existence of these orbits can be properly visualized on a bi-dimensional parameter space, where generally we find *periodic windows*, i.e., continuous sets of parameters, embedded into chaotic regions, for which periodical orbits exist [1, 2]. There is an intricate periodic window, quite general in dynamical systems, whose local nature was explained in [1, 3] but the global features, despite the great number of studies [4–16], remain not well understood. For local and global features we mean typically qualities of an isolated and a multiple periodic windows, respectively. Recently, it has been found that these periodic windows, baptized shrimp [2], are continuously connected along spirals emerging from in a homoclinic bifurcation point [17, 18] (set of parameters for which a bi-asymptotic curve, the homoclinic orbit, converges to a saddle-focus equilibrium point). These spiral structures were verified experimentally in [19, 20] and are also observed in [4, 21, 22].

However, in these researches the distribution of shrimps in the parameter space have not yet been clearly associated to any fundamental dynamical property. To accomplish this, we investigate the relation between the shrimps and the homoclinic curves in the parameter space [23, 24][30]. For the Rössler system, we present a new and remarkable two-parameter space scenery where from each shrimp emerge infinity spirals with focus in discrete points along of a homoclinic bifurcation curve (continuous parameter sets for which homoclinic orbits exist). Each spiral is composed by a shrimp family, i.e., infinite shrimps continuously connected in a spiral sequence. We show that, even the shrimps are a codimension-two phenomena (two parameters are necessary to obtain it), they are accumulating at the spiral focus following scaling laws

predicted by the one-parameter space homoclinic theory [25]. We also show that the reported period adding cascades observed in shrimps accumulations [11, 12] is a consequence of the spiral periodic windows approach to the homoclinic bifurcation point.

Recently was published a work [20] about scaling laws in a electronic homoclinic system where the authors associate scales of tangent bifurcation with the shrimp distribution. Here we discuss this issue in details and show that, in the two-parameter space, the scales measured in shrimps correspond to the distance between crosses of superstable periodic curves. Furthermore, we call the attention to the necessity of a rigorous prove of these scales in shrimp distributions which was done in [26].

In section II we present the spiral scenery of periodic windows, in III we show the scaling laws concerning its distribution and periodicity, and in section IV we present the conclusions.

II. SHRIMP DISTRIBUTIONS

We consider the homoclinic Rössler system given by

$$\begin{aligned}\dot{x} &= -y - z \\ \dot{y} &= x + ay \\ \dot{z} &= bx - cz + xz,\end{aligned}\tag{1}$$

where we fix $b = 0.3$ and analyze the parameter space $c' \times a'$, where $a = a' \sin(\theta) + c' \cos(\theta) + a_0$ and $c = a' \cos(\theta) - c' \sin(\theta) + c_0$ with $a_0 = 0.3301$, $c_0 = 4.9305$, and $\theta = 88.8^\circ$. For the region investigated (Fig. 1) the origin phase space (P_0) is a saddle-focus and the eigenvalues of Eqs. (1) Jacobian matrix evaluated at P_0 are $\lambda_{1,2} = \rho \pm i\omega$ and $\lambda_3 = \lambda$, where λ , ρ , and ω are \mathbb{R}^* .

Periodic and chaotic asymptotic solutions of Eqs. (1) are determined numerically by evaluating the largest nonzero Lyapunov exponent l . In Fig. 1, from black

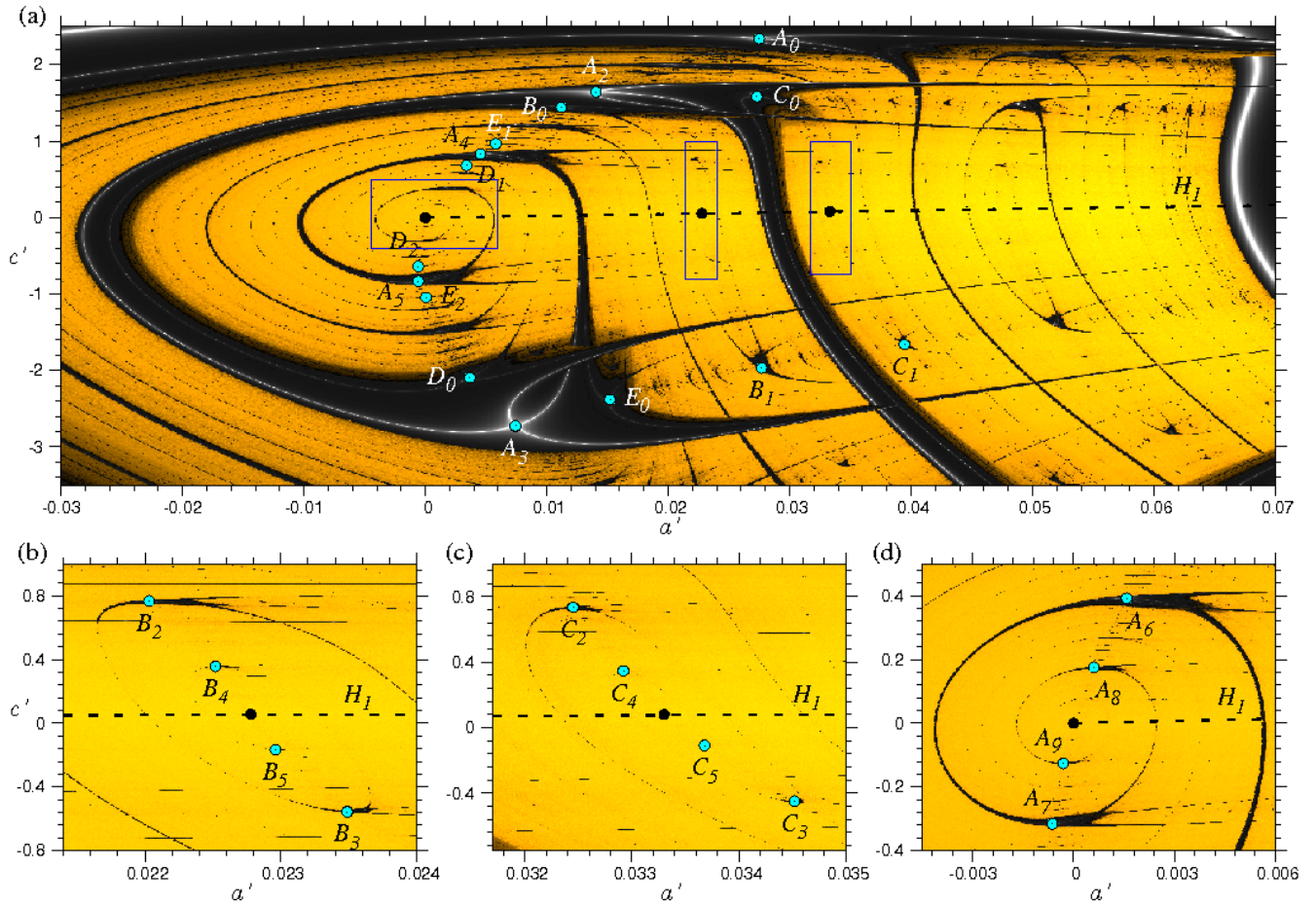


FIG. 1: (Color online) (a) Parameter space $c' \times a'$. The phase space has an chaotic attractor for parameters in yellow and periodic for parameters in gray. The sets A_2 to A_5 are shrimps connected in a spiral way converging asymptotically to the onset of H_1 homoclinic curve (dashed line). B , C , D , and E are shrimp families emerging by flip bifurcations in A_2 and A_3 . The blue square regions are magnified in (b), (c), and (d). The black dots are the spiral focus and the blue dots indicate the shrimp positions.

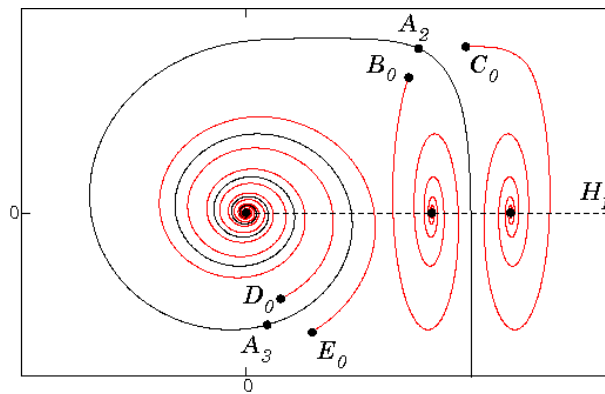


FIG. 2: (Color online) Schematic scenery. Spiral in black corresponds to family A . In red are spirals emerging from shrimps A_2 and A_3 . The dashed line is the H_1 homoclinic bifurcation. The dots along H_1 are the spiral focus points while the points in the spirals represent the crosses of superstables of A_2 , A_3 , B_0 , C_0 , D_0 , and E_0 .

to white ($l < 0$) the periodic orbits increase their stability: in black these orbits bifurcate ($l = 0$) and in white

they are superstable (l achieve the most negative value). Otherwise, from black to yellow ($l > 0$) the behavior is

asymptotically chaotic. The structure labeled A_3 is a particular region of the parameter space where a typical periodic window, the shrimp, can be visualized. The big shadow region, from which extends four narrow antennae, is its *central body* and corresponds to the fundamental periodic window where is the *fundamental periodic orbit* of the shrimp [15]. The central body is bordered by tangent bifurcations, where we find chaotic regions, and by flip bifurcations, where we find sequences of doubled periodic regions with similar shape to the central body. The white lines form the shrimp *skeleton* (parameters set where the periodic regions are around) and represent superstable periodic orbits with behavior strongly attractive. Note that, in the central body, there is a cross between two remarkable superstable curves (blue dots in Fig. 1). We consider this point as a shrimp position and localize it identifying these intersections. In this sense, shrimps are codimension-two structures.

To obtain the parameter sets of the homoclinic bifurcation H_1 associated with the saddle-focus point P_0 , we determine numerically the parameters for which the stable and unstable manifolds of P_0 merge constituting a homoclinic orbit (To obtain homoclinic orbits in piecewise systems, see Ref. [27]). The labels A , B , C , D , and E , in Fig. 1, indicate different shrimp families associated with H_1 . Note that, in each family, shrimps are continuously connected along a spiral sequence around a homoclinic bifurcation point [Typically, two antennae of each shrimp central body is connected with the previous and the next shrimp and the other two antennae connect the shrimp to the divergence region ($a' > 0.2$)]. The index i , in the label families, indicates the element of these sequence. The first shrimp of the sequence is indexed by $i = 1$, the second by $i = 2$, and so on. The index $i = 0$ indicates the structure that connect different families. Thus, B_0 connect family A with family B . Furthermore, excluding the central body of A_2 , for example, B_0 has the same features that characterize family B .

We observe that each shrimp generates many others spiral sequences by flip bifurcations. The central bodies of A_2 and A_3 , in Fig. 1(a), bifurcate in B_0 , C_0 , D_0 , and E_0 , which connect the family A with the families B , C , D , and E . The family B converges to the region close the point ($a' = 0.0228$, $c' = 0.0550$) in an anti-clockwise direction and the family C converges to the region close the point ($a' = 0.0333$, $c' = 0.0800$) in a clockwise direction. Both focus seems to be along the H_1 homoclinic bifurcation curve [see magnifications in Figs. 1(b) and (c)]. The families A , D and E converge to the H_1 onset point (0,0) [see Figs. 1(a) and (d)]. The schematic scenery is shown in Fig. 2. As far we could check, the same is observed in any element of any family suggesting the existence of a fractal structure of spiral self-replications converging asymptotically to the homoclinic bifurcation curve. Moreover, we identify shrimps concentrated in two sets, between the two shrimp antennae that converge to the divergence region (as B and C families), and between two shrimps, i and $i + 2$, of the same family (as D and

E families).

With respect the trajectory behavior, following continuously a shrimp spiral sequence, we observe that the orbit time-period grows smoothly tending to infinity close the homoclinic orbit. So that, the fundamental periodic orbit add one cycle from i -shrimp to the $(i + 2)$ -shrimp forming a period adding cascade accumulating into the H_1 curve, as shown in Figs. 3 (a)-(d). The period adding can be identified considering a flat Poincaré section in $x = 0$ with $y < 0$ close to the plan xy (represented by the dashed lines). The orbits cross the Poincaré section two times in (a), three times in (b), and four times in (c). The homoclinic orbit H_1 has infinite cycles in (d). Note that here we considered A_0 as a shrimp as discussed before.

III. SCALING LAWS FOR SHRIMP DISTRIBUTIONS

Next we analyse our numerical results presented in the last section from the homoclinic theory described by Shilnikov theorem. We focus in the characterization of the two-parameter shrimp structures from these one-parameter theory.

Shilnikov theorem can be applied to systems which saddle-focus equilibrium point have homoclinic orbits (Γ) solutions and, in its normal form, can be represented by

$$\begin{aligned} \dot{x}' &= \rho x' - \omega y' + O(x', y', z') \\ \dot{y}' &= \omega x' + \rho y' + P(x', y', z') \\ \dot{z}' &= -\lambda z' + Q(x', y', z'), \end{aligned} \quad (2)$$

where O , P , and Q are analytic functions with $\dot{O}(\vec{x}') = \dot{P}(\vec{x}') = \dot{Q}(\vec{x}') = 0$, for the equilibrium saddle-focus point $\vec{x}' = 0$, and λ , ρ , and ω are \mathbb{R}_+^* .

If the saddle-focus form Γ with saddle index $\nu < 1/2$ ($\nu = \rho/\lambda$), the Shilnikov Theorem shows that, close to Γ , in a one-parameter space, there are infinite countable sets of periodic and homoclinic bifurcations accumulating into Γ , namely: (I) Stable periodic solutions emerge distributed as $S_p = \lim_{i \rightarrow \infty} (\mu_{i+1}/\mu_i) = \exp -(\pi\rho/\omega)$ where μ_i and μ_{i+1} are two consecutive tangent bifurcation parameters [4, 25, 28]. The period difference between two consecutive periodic orbits is $\Delta T = \lim_{i \rightarrow \infty} (T_{i+1} - T_i) = \pi/\omega$, where T_i is the period of the i -periodic orbit; (II) Infinite classes of homoclinic orbit, characterized by similar orbits, called secondary homoclinic orbits [double-pulse (Γ_2), triple-pulse (Γ_3), and n -pulse (Γ_n)] are distributed following $S_{\Gamma_n} = \lim_{i \rightarrow \infty} (\mu'_{i+1}/\mu'_i) = \exp -(\pi\lambda/\omega)$, where μ'_i and μ'_{i+1} are two consecutive homoclinic bifurcation parameters of Γ_n [29]. The limit $i = \infty$ is related with the primary single-pulse (Γ_1).

To associate the shrimps with this theory, we verify these scaling laws in our numerical simulation. For the family A , the homoclinic orbit parameter is $(a'_\infty, c'_\infty) = (0, 0)$ for which the eigenvalues calculated at the fixed

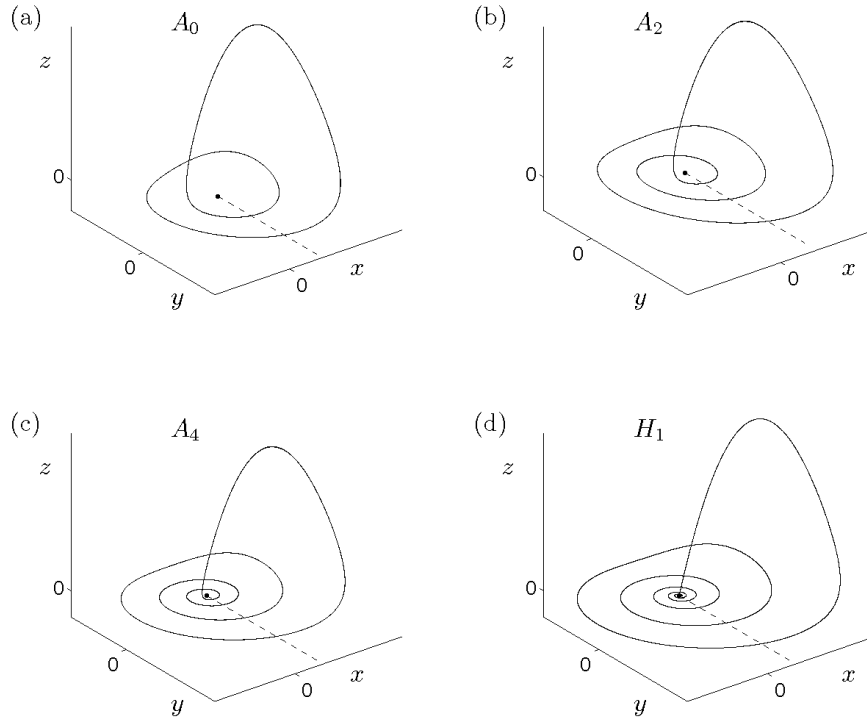


FIG. 3: Period adding of A shrimp family. The periodic trajectories cross the Poincaré section (dashed lines) two, three, four, and infinity times from (a) to (d), respectively.

point P_0 are $\lambda_{1,2} = 0.1354 \pm i0.9867$ and $\lambda_3 = -4.8713$. Thus, the scaling laws are $S_p = 0.6498$, $\Delta T = 3.1840$, and $S_\Gamma \approx 2.10^{-7}$. To measure numerically the periodic orbit scaling S_p , we define $S_i = d_{i+1}/d_i$, with $d_i = [(\tilde{a}'_{i+1} - \tilde{a}'_i)^2 + (\tilde{c}'_{i+1} - \tilde{c}'_i)^2]^{1/2}$, where $(\tilde{a}'_i, \tilde{c}'_i)$ is an intersection point between two superstable curves as de-

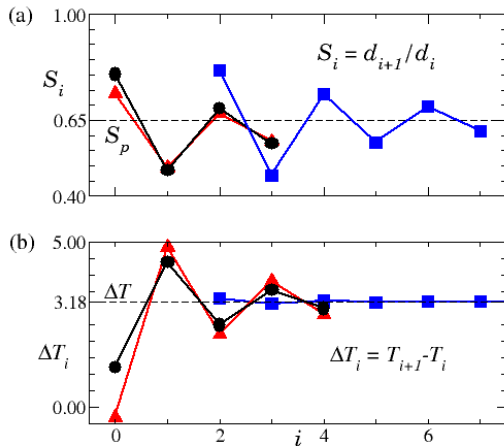


FIG. 4: (Color online) (a) and (b) show, respectively, measure of distribution and difference time-period scalings of shrimps. The dashed lines are the theoretical values, $S_p = 0.6498$ and $\Delta T = 3.1840$, in the limit $i \rightarrow \infty$, of the family A . The symbols square, triangle, and circle are respect families A , B , and C .

finied before the i -shrimp position. The measured S_i for the shrimp family A converges quickly to the theoretical scaling parameter S_p as shown in Fig. 4(a) (curve with square symbol). Figure 4(b) shows that the measured time-period differences $\Delta T_i = T_{i+1} - T_i$ also converge quickly to the theoretical scaling ΔT . Thus, in the limit $i \rightarrow \infty$, the period difference between A_i and A_{i+2} is $2\pi/\omega = 6.3681$. This interval time corresponds to one periodic orbit revolution close to the unstable manifold (plan xy) and explains the period adding phenomenon in homoclinic systems. It suggests that similar mechanism can explain the period adding in other systems. For the family B , we consider $(a'_\infty, c'_\infty) = (0.0228, 0.0550)$. The eigenvalues calculated at P_0 are $\lambda_{1,2} = 0.1524 \pm i0.9831$ and $\lambda_3 = -4.7799$. Thus, the scaling laws are $S_p = 0.6144$, $\Delta T = 3.1956$, and $S_\Gamma \approx 2.10^{-7}$, similarly to the family A . And, for the family C , $(a'_\infty, c'_\infty) = (0.0333, 0.0800)$, $\lambda_{1,2} = 0.1522 \pm i0.9831$ and $\lambda_3 = -4.7910$ with $S_p = 0.6148$, $\Delta T = 3.1955$, and $S_\Gamma \approx 2.10^{-7}$. The scalings S_i and ΔT_i of B and C families are in agreement to the theoretical estimated S_p and ΔT as shown in Fig. 4(a) and (b) (triangle and circle symbols for B and C families, respectively). Although the homoclinic scaling law parameter is very low for being verified numerically, we have observed the existence of many different bifurcations H_n close to the primary H_1 homoclinic curve parameter. The scalings measured of families D and E have values very similar to the family A and it was omitted in Fig. 4.

We emphasize that it is not expected that the scaling laws here considered match with the shrimps scalings, since shrimps are a codimension-two phenomena. Our results suggest strongly that shrimps are distributed along lines in regions close to the homoclinic orbit bifurcation [See Figs. 1 (b)-(d)].

IV. CONCLUSIONS

We used the knowledge of homoclinic orbits distribution in the bi-dimensional parameter space to explain the distribution of periodic windows in this space. We found infinite periodic structures with spiral shape distributed along the homoclinic bifurcation curve H_1 . Each spiral has two extremities: one is a point in H_1 , which is its focus, and the other is a shrimp. In the other side, from each shrimp derive infinite spirals with different focus along H_1 . Thus, the spiral are composed by infinite shrimps, which compose infinite spirals which have infinite shrimps which compose infinite spirals and son on. This characterize the fractality of this scenery of spirals.

It is worth to mention that, excluding family A , each spiral is composed by a family of shrimps that, close the H_1 curve, the shape of its orbit in the phase space ap-

proaches the shape of an secondary homoclinic orbit Γ_n (also called subsidiary homoclinic orbit). It suggest that the real focus of each spiral is a point close H_1 where is formed a Γ_n orbit. As discussed before, the classes of homoclinic orbit are organized close H_1 following the scale S_{Γ_n} . Thus we argue that the spiral distribution in the parameter space should follows the scale S_{Γ_n} .

We have also identified properties of the homoclinic theory in the shrimps organization. We notice that this result is not expected since the homoclinic scalings are valid just in a one-parameter space and shrimps are two-parameter structures. It indicates that shrimps, close to the homoclinic bifurcation, are organized along a line that intersects H_1 . The analytical prove of this is merit of investigation [26].

Acknowledgments

We would like to thank Dr. Adilson E. Motter for important comments and suggestions about this paper, Dr. Manuel A. Matías for helpful discussions about bifurcation theory and Prof. Jason Gallas for previous discussions about shrimp properties. This research has a financial support of FAPESP and CNPq.

-
- [1] S. Fraser, R. Kapral, Phys. Rev. A 25 (1982) 3223.
 - [2] J. A. C. Gallas, Phys. Rev. Lett. 70 (1993) 2714.
 - [3] J. A. C. Gallas, Physica A 202 (1994) 196.
 - [4] P. Gaspard, R. Kapral, G. Nicolis, J. Stat. Phys. 35 (1984) 697.
 - [5] S. Fraser, R. Kapral, Phys. Rev. A 30 (1984) 1017.
 - [6] C. Mira, Chaotic dynamics, World Scientific, Singapore, 1987.
 - [7] K. Ullmann, I. L. Caldas, Chaos, Solitons and Fractals 7 (1996) 1913.
 - [8] M. S. Baptista, I. L. Caldas, Int. J. Bifurcation Chaos 7 (1997) 447.
 - [9] L. Glass, Nature 410 (2001) 277.
 - [10] C. Bonatto, J. C. Garreau, J. A. C. Gallas, Phys. Rev. Lett. 95 (2005) 143905.
 - [11] C. Bonatto, J. A. C. Gallas, Phys. Rev. E 75 (2007) 055204.
 - [12] C. Bonatto, J. A. C. Gallas, Philos. Trans. R. Soc. A 366 (2008) 505.
 - [13] O. C. D. Cardoso, H. A. Albuquerque, R. M. Rubinger, Phys. Lett. A 373 (2009) 2050.
 - [14] H. A. Albuquerque, P. C. Rech, Int. J. Bifurcation Chaos 19 (2009) 1351.
 - [15] E. N. Lorenz, Physica D 237 (2008) 1689.
 - [16] E. S. Medeiros, S. L. T. de Souza, R. O. Medrano-T, I. L. Caldas, Phys. Lett. A 374 (2010) 2628.
 - [17] O. Feo, G. M. Maggio, M. P. Kennedy, Int. J. Bifurcation Chaos 10 (2000) 935.
 - [18] C. Bonatto, J. A. C. Gallas, Phys. Rev. Lett. 101 (2008) 054101.
 - [19] O. De Feo, G. M. Maggio, Int. J. Bifurcation Chaos 13 (2003) 2917.
 - [20] R. Stoop, P. Benner, Y. Uwate, Phys. Rev. Lett. 105 (2010) 074102.
 - [21] L. van Veen, D. Liley, Phys. Rev. Lett. 97 (2007) 208101.
 - [22] H. A. Albuquerque, R. M. Rubinger, P. C. Rech, Phys. Lett. A 372 (2008) 4793.
 - [23] R. O. Medrano-T, COMPLEX SYSTEMS 2008, <http://www.lac.inpe.br/WSACS/programme.jsp>, 2008.
 - [24] R. O. Medrano-T, I. L. Caldas, Dynamics Days South America 2010, <http://urlib.net/sid.inpe.br/mte-m19@80/2010/08.11.01.46>, 2010.
 - [25] Y. A. Kuznetsov, Elements of applied bifurcation theory, Springer, United States of America, 2004.
 - [26] R. O. Medrano-T, I. L. Caldas (in preparation).
 - [27] R. O. Medrano-T, M. S. Baptista, I. L. Caldas, Physica D 186 (2003) 133.
 - [28] P. Glendinning, C. Sparrow, J. Stat. Phys. 35 (1984) 645.
 - [29] R. O. Medrano-T, M. S. Baptista, I. L. Caldas, Chaos 15 (2005) 033112.
 - [30] The final program of [23] can be accessed at: <http://www.lac.inpe.br/WSACS/imagens/ProgramaWeb.pdf>